


Article

# Stearic Acid, Beeswax and Carnauba Wax as Green Raw Materials for the Loading of Carvacrol into Nanostructured Lipid Carriers

Juliana G. Galvão <sup>1</sup>, Raquel L. Santos <sup>1</sup>, Ana Amélia M. Lira <sup>1</sup>, Renata Kaminski <sup>2</sup>, Victor H. Sarmiento <sup>2</sup>, Patricia Severino <sup>3,4,5</sup> , Silvio S. Dolabella <sup>6</sup>, Ricardo Scher <sup>6</sup>, Eliana B. Souto <sup>7,8,\*</sup> and Rogéria S. Nunes <sup>1,\*</sup>

<sup>1</sup> Department of Pharmacy, Federal University of Sergipe, São Cristóvão 49100-000, Brazil; julianaggalvao@gmail.com (J.G.G.); raquel.lines@hotmail.com (R.L.S.); ana\_lira2@hotmail.com (A.A.M.L.)

<sup>2</sup> Department of Chemistry, Federal University of Sergipe, Itabaiana 49100-000, Brazil; re\_kaminski@hotmail.com (R.K.); vhsarmiento@gmail.com (V.H.S.)

<sup>3</sup> Laboratory of Nanotechnology and Nanomedicine (LNMED), Tiradentes University, Institute of Technology and Research (ITP), Aracaju 49010-390, Brazil; pattypharma@gmail.com

<sup>4</sup> Instituto de Tecnologia e Pesquisa (ITP), Av. Murilo Dantas, Aracaju 49032-490, Brazil

<sup>5</sup> Tiradentes Institute, Boston, MA 02125, USA

<sup>6</sup> Department of Morphology, Federal University of Sergipe, São Cristóvão 49100-000, Brazil; dolabellaufs@gmail.com (S.S.D.); rica.scher@gmail.com (R.S.)

<sup>7</sup> Department of Pharmaceutical Technology, Faculty of Pharmacy, University of Coimbra, 3000-548 Coimbra, Portugal

<sup>8</sup> CEB—Centre of Biological Engineering, University of Minho, Campus de Gualtar, 4710-057 Braga, Portugal

\* Correspondence: ebsouto@ff.uc.pt (E.B.S.); rogeria.ufs@hotmail.com (R.S.N.)

Received: 13 August 2020; Accepted: 7 September 2020; Published: 9 September 2020



**Abstract:** The use of lipid nanoparticles as drug delivery systems has been growing over recent decades. Their biodegradable and biocompatible profile, capacity to prevent chemical degradation of loaded drugs/actives and controlled release for several administration routes are some of their advantages. Lipid nanoparticles are of particular interest for the loading of lipophilic compounds, as happens with essential oils. Several interesting properties, e.g., anti-microbial, antitumoral and antioxidant activities, are attributed to carvacrol, a monoterpenoid phenol present in the composition of essential oils of several species, including *Origanum vulgare*, *Thymus vulgaris*, *Nigella sativa* and *Origanum majorana*. As these essential oils have been proposed as the liquid lipid in the composition of nanostructured lipid carriers (NLCs), we aimed at evaluating the influence of carvacrol on the crystallinity profile of solid lipids commonly in use in the production of NLCs. Different ratios of solid lipid (stearic acid, beeswax or carnauba wax) and carvacrol were prepared, which were then subjected to thermal treatment to mimic the production of NLCs. The obtained binary mixtures were then characterized by thermogravimetry (TG), differential scanning calorimetry (DSC), small angle X-ray scattering (SAXS) and polarized light microscopy (PLM). The increased concentration of monoterpenoid in the mixtures resulted in an increase in the mass loss recorded by TG, together with a shift of the melting point recorded by DSC to lower temperatures, and the decrease in the enthalpy in comparison to the bulk solid lipids. The miscibility of carvacrol with the melted solid lipids was also confirmed by DSC in the tested concentration range. The increase in carvacrol content in the mixtures resulted in a decrease in the crystallinity of the solid bulks, as shown by SAXS and PLM. The decrease in the crystallinity of lipid matrices is postulated as an advantage to increase the loading capacity of these carriers. Carvacrol may thus be further exploited as liquid lipid in the composition of green NLCs for a range of pharmaceutical applications.

**Keywords:** carvacrol; stearic acid; beeswax; carnauba wax; nanostructured lipid carriers; crystallinity

## 1. Introduction

Carvacrol (or cymophenol) is chemically known as 5-isopropyl-2-methylphenol and is obtained from a range of aromatic plants such as oregano (*Origanum vulgare* L.), marjoram (*Origanum majorana* L.), black cumin (*Nigella sativa* L.) or thyme (*Thymus vulgaris* L.) [1,2]. Pharmacological properties, such as antioxidant [3,4], anti-inflammatory [5], analgesic [6], antitumor [7], antimicrobial [8] and antiprotozoal activities [9–11], have been attributed to this phenolic monoterpene. Its use in clinical settings is, however, compromised by its lipophilic character, resulting in low aqueous solubility, risk of oxidation and also high volatility [1]. The loading of carvacrol in lipid nanoparticles may be a promising strategy to reduce its volatility and improve its loading and bioavailability [12]. Only a limited number of studies have reported the loading of carvacrol into nanoparticles [13,14], while none has yet reported the use of nanostructured lipid carriers (NLCs) for this purpose.

It has already been demonstrated that lipid mixtures have a great impact on the chemical stability of volatile compounds [15–18]. Among lipid nanoparticles, NLCs are attractive colloidal carriers as they consist of nanosized particles based on a blend of solid and liquid lipids dispersed in an aqueous surfactant solution [19–22]. The combined ratio between solid and liquid lipid should ensure that the produced lipid matrix melts above 40 °C [20,23]. Besides being biodegradable, biocompatible and of low toxicity, the major advantages of NLCs include their green nature, capacity for protecting loaded drugs/actives from chemical degradation and the provision of a controlled release of the payload [19,24–29]. Due to their nanostructured matrix, obtained by disrupting the crystal packing of the solid lipid by mixing it with a liquid lipid, NLCs may also offer a triggered release [30]. The degrees of crystallization and polymorphism of the NLC matrices are strongly dependent on the ratio between the solid and liquid lipids [31]. A low degree of crystallinity of the matrix is usually associated with a higher payload. The use of lipid mixtures that crystallize in a less organized matrix is linked to higher loading capacity of the nanocarriers.

Several lipids excipients can be used for the production of NLCs, among which fatty acids (e.g., palmitic acid, stearic acid), fatty alcohols, mono-, di- and triglycerides, vegetable oils and waxes (e.g., carnauba wax, beeswax, cetyl palmitate) are the most frequently used [32–34]. In pharmaceutical products, the employment of natural lipids is desirable [35].

Stearic acid is a saturated 18-carbon chain fatty acid that melts around 69 °C and is obtained from both animal and vegetal sources. It shows higher in vivo tolerability and less toxicity than fats from synthetic origin [36,37]. Beeswax is a natural fatty material with a melting point ranging between 61 °C and 67 °C, obtained from the combs of bees (*Apis mellifera*) [38,39]. Carnauba wax is a plant exudate from the Brazilian “tree of life” (*Copernicia cerifera*), composed almost entirely of wax acid esters of C24 and C28 carboxylic acids and saturated long-chain mono-functional alcohols, that melts around 82 °C, thus showing high crystallinity [40]. Stearic acid, beeswax and carnauba wax have been selected as they are considered non-toxic and “generally recognized as safe” (GRAS) by the US Food and Drug Administration (FDA). The use of these three fats in the production of drug delivery systems has also been previously described [41,42].

Since the majority of methods used for the production of NLCs require heating, the volatility of carvacrol may compromise the loading capacity and encapsulation efficiency of the particles for the monoterpene. The liquid status of carvacrol may also affect the structure of the lipid matrix. The aim of this study was to evaluate the effect of carvacrol and its concentration on the crystallinity profile of lipid mixtures commonly used for the production of NLCs. Such lipid screening is commonly recommended prior to the development of NLCs, for the selection of the best lipid/lipid combination to achieve high payloads. Thermogravimetry (TG), differential scanning calorimetry (DSC), small-angle X-ray scattering (SAXS) and polarized light microscopy (PLM) were used for the physicochemical characterization of the lipid mixtures.

## 2. Material and Methods

### 2.1. Materials

Beeswax and carnauba wax were purchased from GM Ceras (São Paulo, Brazil). Stearic acid was obtained from Dinâmica<sup>®</sup> (Diadema, São Paulo, Brazil). Carvacrol (5-isopropyl-2-methylphenol, CAS Number 499-75-2) was purchased from Sigma-Aldrich<sup>®</sup> (St. Louis, MO, USA).

### 2.2. Preparation of the Binary Mixtures

Prior to the preparation of the binary mixture, the selected solid lipids, stearic acid (SA), beeswax (BW) and carnauba wax (CW), were first heated above their melting points, i.e., 58 °C, 63 °C and 82 °C, respectively, followed by cooling down to allow them to recrystallize [43]. To prepare the binary mixtures containing 10%, 25% and 50% of carvacrol, the solid lipids (SA, BW, CW) and carvacrol were melted at a temperature of 85 °C, were mechanically mixed for 5 minutes and then cooled down under continuous stirring until solidification. Composition of the binary mixtures is depicted in Table 1. The freshly prepared mixtures were then characterized.

**Table 1.** Composition of the binary mixtures (% m/m).

Samples	Carvacrol (mg)	Stearic Acid (mg)	Beeswax (mg)	Carnauba Wax (mg)
SA 10%	0.10	0.90	—	—
SA 25%	0.25	0.75	—	—
SA 50%	0.50	0.50	—	—
BW 10%	0.10	—	0.90	—
BW 25%	0.25	—	0.75	—
BW 50%	0.50	—	0.50	—
CW 10%	0.10	—	—	0.90
CW 25%	0.25	—	—	0.75
CW 50%	0.50	—	—	0.50

### 2.3. Thermogravimetric (TG) Analysis

Thermogravimetric (TG) analysis was performed to evaluate the mass loss under heating, which was recorded in a Q50 TG (TA Instruments, New Castle, Delaware, USA). Samples of approximately 10 mg were heated up from 25 °C to 600 °C, applying a heating rate of 10 °C/min, under a dynamic argon atmosphere (50 mL/min) in platinum crucibles.

### 2.4. Differential Scanning Calorimetry (DSC) Analysis

Differential scanning calorimetry (DSC) analysis was performed to record the melting events and calculate the melting enthalpy using a DSC Q20 (TA Instruments, New Castle, Delaware, USA). Samples of approximately 3 mg were heated up from 25 °C to 100 °C, under a heating rate of 10 °C/min and dynamic argon atmosphere (50 mL/min) in aluminum crucibles.

### 2.5. Small-Angle X-ray Scattering (SAXS) Analysis

Small-angle X-ray scattering (SAXS) analysis was carried out to evaluate the polymorphism of the lipid mixtures. Diffractograms were obtained on the D1B-SAXS1 beamline at the Brazilian Synchrotron Light Laboratory (LNLS, Campinas, Brazil). Measurements were performed at room temperature, using a silicon-W/B4C toroidal multilayer mirror, collimated by a set of slits defining a pinhole geometry, at a wavelength of  $k = 1.499 \text{ \AA}$  and detected on a Pilatus 300 k detector (Dectris Ltd., Baden-Dättwil, Switzerland). The sample-to-detector distance was 814 mm, covering a scattering vector “ $q$ ” ( $q = (4\pi/\lambda)\sin\theta$ ) and ranging from 0.1 to 4.0 nm, where  $2\theta$  is the scattering angle. A standard silver behenate powder was measured to calibrate the sample-to-detector distance, detector tilt and

direct beam position (at room temperature). From the total scattering intensity, the parasitic scattering produced was subtracted.

### 2.6. Polarized Light Microscopy (PLM) Analysis

The melted SA, BW, CW and their mixtures with carvacrol (Table 1) were examined under polarizing light with an Olympus model BX-51 microscope (Tokyo, Japan), coupled to a digital LC Color Evolution (PL-A662) camera. The software PixeLINK (Gloucester, Ontario, Canada) was used for recording the images. Briefly, the samples were heated above the melting point, placed between two glass plates and allowed to recrystallize by cooling down to room temperature. They were then analyzed under PLM at room temperature (25 °C). All samples were checked using 20× magnification.

## 3. Results and Discussion

For the development of stable NLC formulations, the evaluation of the degree of crystallinity and polymorphism of the lipid matrices is instrumental to ensure that the matrix remains in the solid state at room temperature. Besides, it is possible to predict polymorphic changes and the degree of miscibility between the solid lipid and the liquid lipid during recrystallization [35,44].

As for the NLC production, the methods usually require heating and the volatility of carvacrol compromises the success of its loading in the lipid matrices. TG analysis can be useful to determine the mass change after the tempering process. Figure 1 shows the mass change (%) of selected solid lipids (SA, BW and CW) and their respective binary mixtures containing 10, 25 and 50% of carvacrol, as a function of temperature.

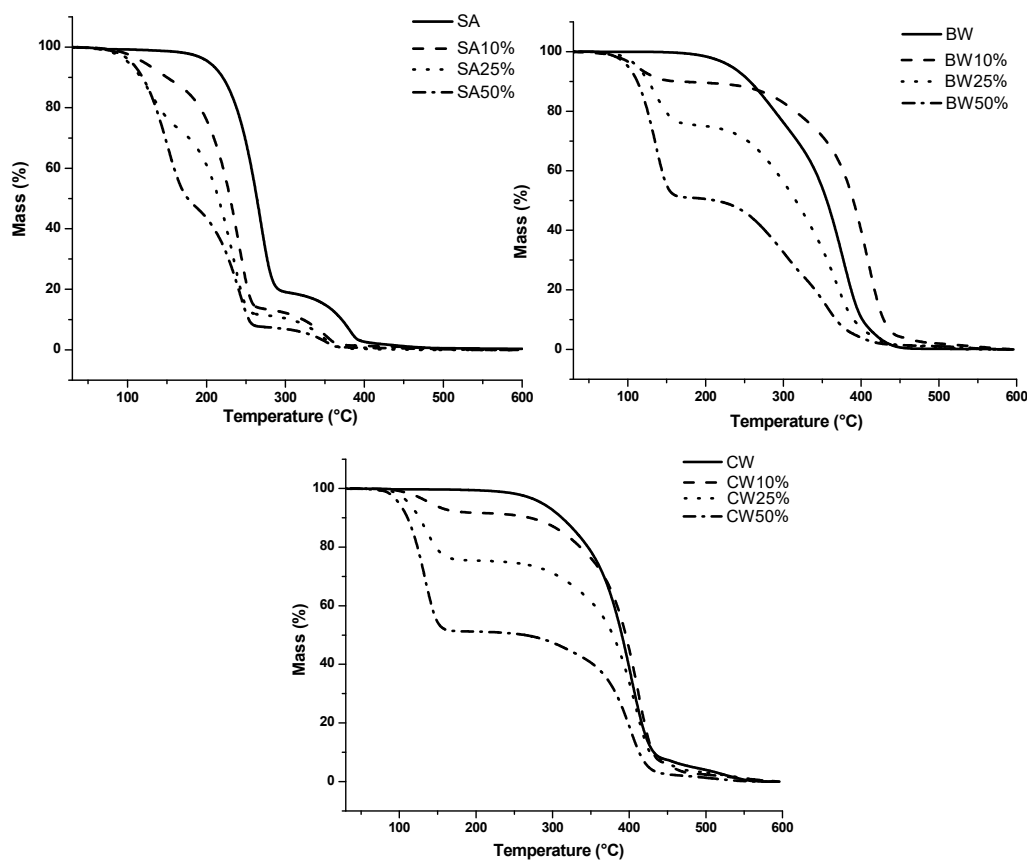


**Figure 1.** Thermogravimetric curves of the stearic acid (SA, upper left), beeswax (BW, upper right) and carnauba wax (CW, bottom) in comparison to their binary mixtures containing 10%, 25% and 50% of carvacrol (see Table 1 for composition).

Two mass loss events were identified in the differential thermogravimetric (DTG) curve of stearic acid (SA, Figure 1), the first being within the temperature range of 161 and 306 °C ( $\Delta m_1 = 79.63\%$   $T_{peak}$  DTG  $\sim 267$  °C), which is typical of the SA decomposition, and the second within the range of 306 and 410 °C, attributed to the elimination of carbonaceous material [45,46]. The TG curves of beeswax (Figure 1, upper right) and carnauba wax (Figure 1, bottom) depict only one mass loss event within the temperature range of 180–480 °C ( $\Delta m_1 = 99.5\%$   $T_{peak}$  DTG  $\sim 396.7$  °C) and 250–500 °C ( $\Delta m_1 = 98.5\%$   $T_{peak}$  DTG  $\sim 426.1$  °C), respectively. The analysis of the binary mixtures shows the detection of carvacrol during the progressive mass loss with the increasing concentration of the oil and over the course of the experiment. It was interesting to see that the first mass loss event observed for all samples was within the range of the percentage of carvacrol (10%, 25% and 50%) in each of the binary mixtures (Table 2).

**Table 2.** Thermogravimetric data recorded for the first mass loss of the solid lipids (SA, BW and CW) containing 10%, 25% and 50% of carvacrol (see Table 1 for composition).

Samples	1st Loss in Mass $\Delta m$ (%)
SA 10%	10.40%
SA 25%	24.44%
SA 50%	49.48%
BW 10%	9.66%
BW 25%	23.74%
BW 50%	47.84%
CW 10%	7.82%
CW 25%	24.20%
CW 50%	48.07%

Despite the volatility of the monoterpene [47], the results shown in Figure 1 demonstrate that when mixing carvacrol with the three solid lipids in the selected ratios, no mass change was recorded within the range of temperatures below 100 °C. This result assures the possibility of producing NLCs for the loading of carvacrol, since the production methods do not make use of temperatures above 100 °C. Carvacrol is an oil at room temperature (melting point of 1 °C, boiling point of 237.7 °C). No chemical degradation of carvacrol is thus anticipated from the thermal stress during the production of the melted mixtures.

DSC analysis provided information about the physical state of the melted lipids and their mixtures with carvacrol, degree of crystallinity, melting temperatures and respective enthalpies [48]. Figure 2 shows the DSC curves for the selected solid lipids (SA, BW and CW) and their binary mixtures containing 10%, 25% and 50% of carvacrol.

As seen in Figure 2 (left panel), SA showed an endothermic event between 40 °C and 65 °C (with the  $T_{peak} \sim 57$  °C), which is related to the melting point of the solid lipid [45,46]. The melting point of beeswax was recorded at  $T_{peak} \sim 63$  °C (middle panel) and that of carnauba wax was recorded at  $T_{peak} \sim 82$  °C (right panel). The adding of monoterpene to the bulk lipids resulted in a slight shift down to lower temperatures, i.e., from 57 °C down to 56.34 °C, 54.9 °C and 50.2 °C, for stearic acid with 10%, 25% and 50% of carvacrol, respectively (Figure 2, left). Shifts in the melting points were also recorded for BW down to 61.4 °C, 58.5 °C and 50.9 °C, and for CW down to 81.36 °C, 77.3 °C and 72.9 °C, when added with 10%, 25% and 50% carvacrol, respectively.

The decrease in the enthalpy, which is the amount of heat involved in thermal events, was compared among the three solid lipids when increasing the concentration of carvacrol (Figure 3). When compared to pure solid lipids, the increase in the carvacrol content (10%, 25% and 50%) induced a decrease in the endothermic events related to melting and therefore the related enthalpy. Severino et al. studied the influence of the loading of capric/caprylic triglyceride mixtures (liquid lipid) in stearic acid matrices [37], demonstrating that the increase in melting enthalpy and crystallization was inversely proportional to the amount of oil in the formulation. A decrease in the crystallinity and melting enthalpy was observed,

which translates a higher disorder of the lipid lattice [37]. Similar results were described when mixing theobroma oil and beeswax, contributing to the nanostructuring of the lipid matrix towards a greater disorder [35]. A less ordered matrix favors a higher loading capacity for active ingredients due to the increased number of voids and vacancies able to accommodate a higher number of molecules in the structure of the lattice. Due to the liquid character of carvacrol, its presence is likely to delay the complete crystalline rearrangement of the solid lipids.

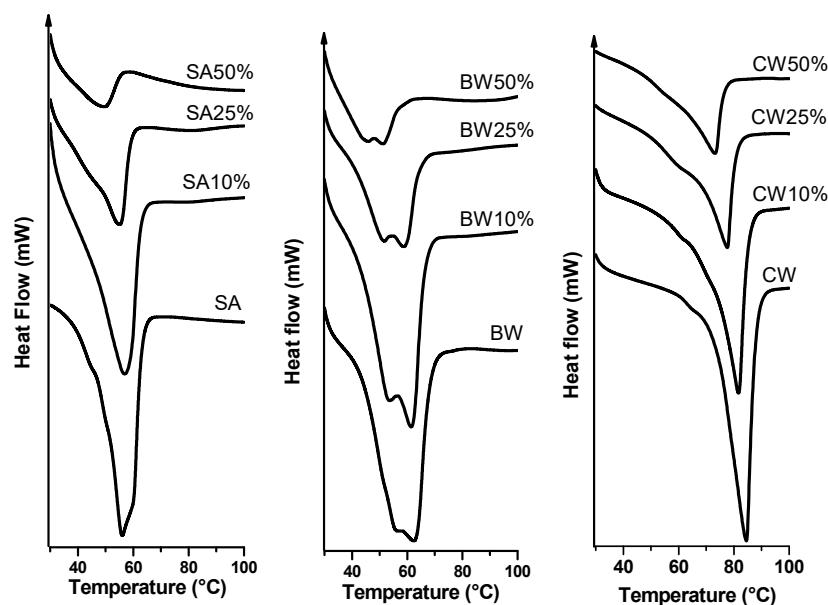


**Figure 2.** Differential scanning calorimetry curves of the stearic acid (left, SA), beeswax (middle, BW) and carnauba wax (right, CW), in comparison to their binary mixtures containing 10%, 25% and 50% of carvacrol (see Table 1 for composition).

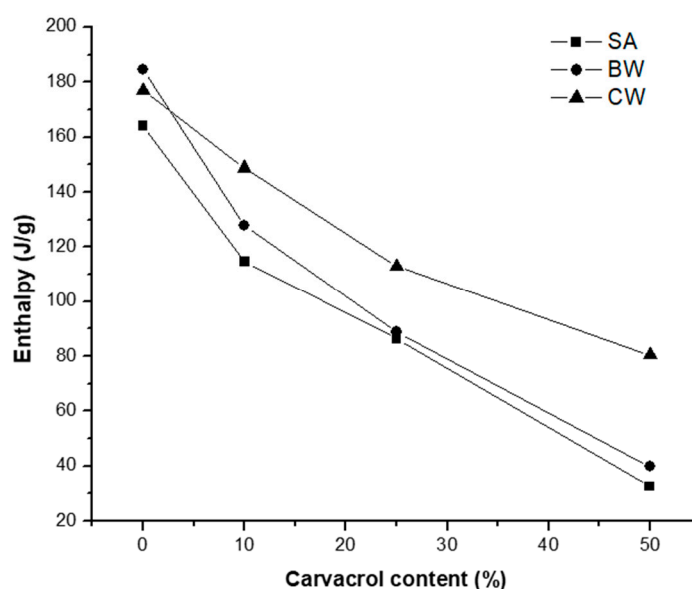


**Figure 3.** Variation of the enthalpy of stearic acid (SA), beeswax (BW) and carnauba wax (CW) with the increased concentration of carvacrol (% w/w) in each binary mixture.

A depression in the melting point of the bulk solid lipids was detected upon the increased addition of carvacrol to all three solid lipids. The decrease in the melting peak ( $T_{peak}$ ), onset temperature,

enthalpy and the increase in the width of the melting event (WME) of SA, BW and CW when 10%, 25% and 50% of carvacrol was added to the solid lipids demonstrates that monoterpene is miscible in the tested concentration range with the three solid lipids (Table 3). Kasongo et al. [44] has reported similar results for the adding of Transcutol® HP up to 20% (w/w) to the solid lipid Precirol® ATO 5.

**Table 3.** Melting peak, onset temperature and width of the melting event of the bulk solid lipids and their binary mixtures with carvacrol obtained by differential scanning calorimetry (see Table 1 for composition).

Samples	Melting Peak (°C)	Onset (°C)	Width of Melting Event <sup>1</sup> (°C)
Bulk SA	57.0	37.0	28.0
SA 10%	56.5	36.0	29.0
SA 25%	54.9	34.3	30.0
SA 50%	50.2	34.0	30.0
Bulk BW	63.0	55.8	32.6
BW 10%	61.4	50.0	32.7
BW 25%	58.5	48.1	32.7
BW 50%	50.9	48.0	24.5
Bulk CW	82.0	39.5	35.5
CW 10%	81.4	38.6	36.5
CW 25%	77.3	38.2	37.1
CW 50%	72.9	36.2	39.2

<sup>1</sup> WME, width of the melting event, i.e., difference between endset and onset temperatures.

The same samples were also analyzed by SAXS, for the recording of the polymorphic changes of the bulk solid lipid with the addition of 10%, 25% and 50% of carvacrol (Figure 4).

Bulk SA showed five peaks at  $q$  ( $\text{nm}^{-1}$ ) of 1.27, 1.53, 2.25, 3.06 and 3.84, which are typical of highly ordered materials (Figure 4, upper left). Both waxes (BW and CW) exhibited peaks with a periodicity, typical of lamellar structures (1:2:3:4 . . . ) [49]. With the increasing concentration of carvacrol, some peaks disappeared and/or had lower intensity of some of the solid lipid characteristic peaks, suggesting that monoterpene decreased the structure ordering of the bulks, confirming the DSC results [43]. Attama et al. also reported a lamellar crystal arrangement for beeswax [35].

Figure 5 shows the lattice spacing “ $d$ ” as a function of carvacrol concentration [50]. Lattice spacing “ $d$ ” was determined using the equation  $d = 2\pi/q$ . When increasing the concentration of carvacrol, the bulk SA did not show any changes in the lattice spacing (which remained  $d \sim 4$  nm). For both waxes (BW and CW), the “ $d$ ” value increased with the increase in monoterpene concentration. Bragg’s equation ( $2d \cdot \sin\theta = n\lambda$ ) was used to determine the interlayer distance ( $d$ ) in the lipid lattice, where  $\theta$  is the angle of diffraction,  $\lambda$  the wavelength and  $n$  the order of the crystalline plane [51]. When compared with the bulk lipid, the increase in the distance with the loading with a drug, anticipates the assumption that the drug molecules are within the lipid lattice. As shown in the patterns of Figure 5, the experimental lattice spacing of bulk stearic acid, beeswax and carnauba wax was, respectively, 4.15 nm, 7.25 nm and 8.50 nm. The mixing with increasing concentrations of carvacrol increased the interlayer spacing of beeswax and carnauba wax, but not of stearic acid. This result anticipates the assumption that both waxes would improve the loading capacity (LC) and encapsulation efficiency (EE) of carvacrol in NLCs composed of one of those lipids. The higher the concentration of carvacrol in the wax mixtures, the higher the lamellar spacing and thus the higher the LC and EE. According to Alexandridis et al., the amount of interface (and lamellae) decreases with the increase in the “ $d$ ” value and, thus, increases the spacing between lamellae [50]. This result indicates that carvacrol is most likely to be placed in between the solid lipid lamellae of both waxes, increasing the “ $d$ ” value, thus promoting a less ordered structure, which also confirms the DSC results. An amorphous polymorphic form ( $\alpha$ -form) is associated with a less ordered structure of the lipid core, thus also improving both LC and EE [52].

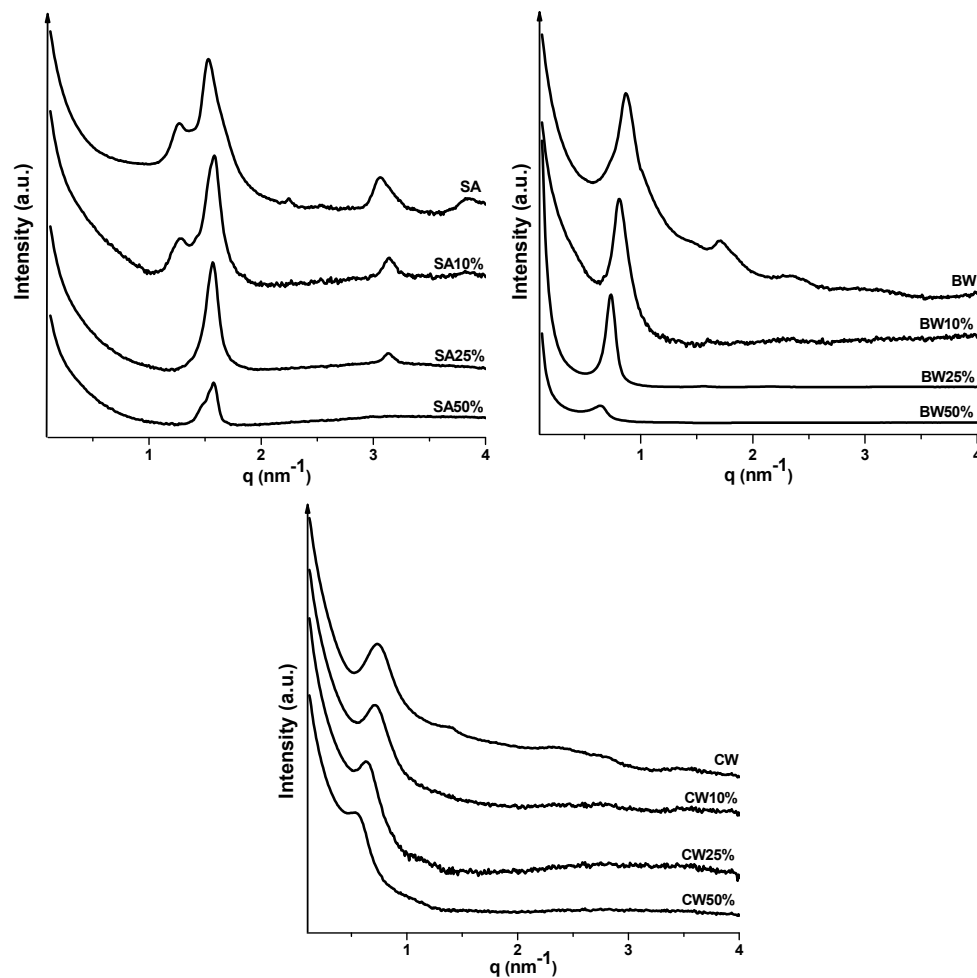


**Figure 4.** Scattering X-ray diffraction patterns  $I(q)$  as a function of scattering vector ( $q$ ) for stearic acid (SA, upper left), beeswax (BW, upper right), carnauba wax (CW, bottom) and their binary mixtures containing 10%, 25% and 50% of carvacrol (see Table 1 for composition).

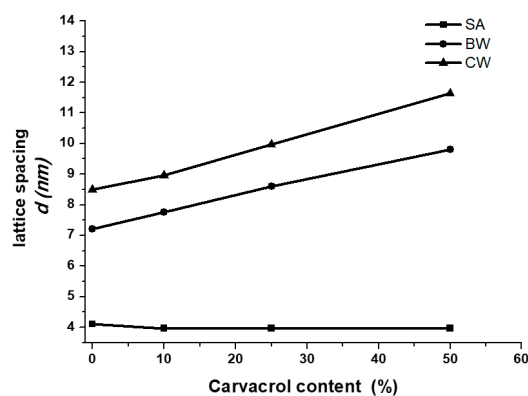


**Figure 5.** Value of lattice spacing “ $d$ ” measured by small-angle X-ray scattering of bulk solid lipids (stearic acid, beeswax and carnauba wax) plotted as a function of carvacrol concentration (10%, 25% and 50%).

The optical behavior of solid lipids and their mixtures with carvacrol was checked by PLM. Materials can be classified either as anisotropic or as isotropic, depending on the effect that the material causes under polarized light. In the characterization of solid lipids, PLM can be used to observe microstructural changes [35].



Figure 6 shows the optical micrographs recorded at room temperature of bulk lipids (SA, BW and CW) and their binary mixtures with increased concentration of carvacrol (10%, 25% and 50%). The bulk solid lipids showed highly ordered crystalline microstructures, as previously demonstrated by DSC and SAXS analysis. SA exhibited a needle-shaped structure, while both waxes (BW and CW) clearly showed a maltese cross symbol of lamellar structure, confirming the results recorded with SAXS [43]. The addition of 10%, 25% and 50% of carvacrol resulted in a decrease in the size and thickness of these compared to the pure solid lipids (SA, BW and CW), suggesting a lower crystallinity. These results are in agreement with Gaillard et al., who showed that the crystallinity degree of beeswax decreased with an increase in the content of rosin [39].

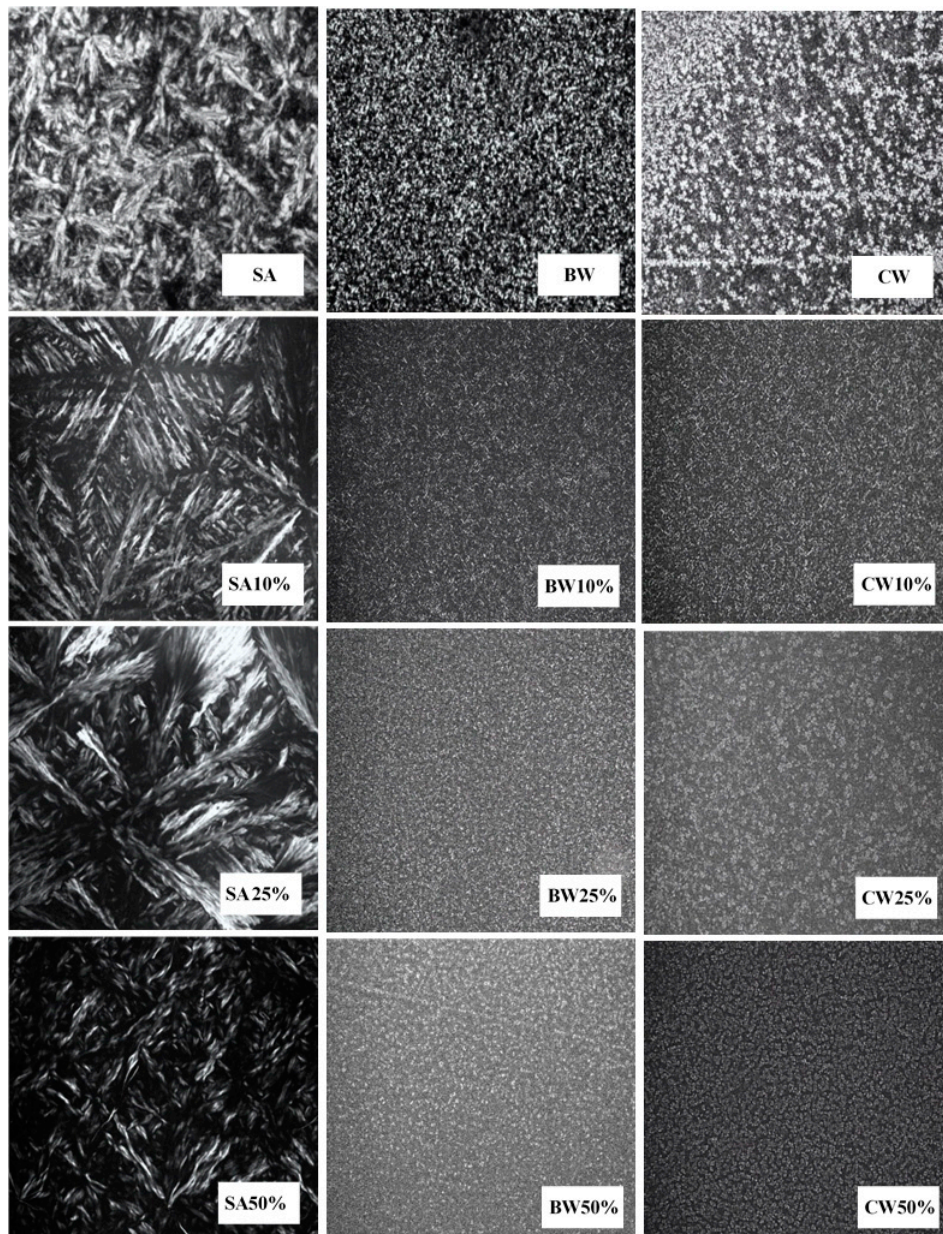


**Figure 6.** Optical micrographs produced with polarized light microscopy at room temperature corresponding to stearic acid, beeswax, carnauba wax and their binary mixtures containing 10%, 25% and 50% of carvacrol. Images obtained using 10 × magnification.

#### 4. Conclusions

Due to the biological properties of carvacrol, this monoterpene has potential to be used as an active ingredient in pharmaceutical formulations; its oily liquid character makes this compound a suitable ingredient in formulating nanostructured lipid carriers (NLCs). Carvacrol was found to be well mixed with melted stearic acid, beeswax and carnauba wax, while the binary mixtures resulted in less ordered structures, which can be further exploited as drug delivery carriers. It is hypothesized that lipid mixtures containing 10%, 25% and 50% w/w of carvacrol in the solid lipids (SA, BW, and CW) can be used to obtain NLCs. Lower melting temperatures and enthalpy were recorded when adding the monoterpene to the three bulk lipids (confirmed by DSC). SAXS and PLM analyses demonstrated the presence of less ordered structures of the binary mixtures in comparison to the bulk counterparts. These binary mixtures can thus be explored in the production of NLCs for drug delivery.

**Author Contributions:** V.H.S., P.S., S.S.D., R.S. and R.S.N. contributed to the conceptualization, methodology, validation, formal analysis and investigation; J.G.G., R.L.S., A.A.M.L., R.K. and E.B.S. contributed to the writing—original draft preparation; E.B.S., P.S. and R.S.N. contributed to supervision, writing—review and editing, project administration, resources and funding acquisition. All authors have made a substantial contribution to the work. All authors have read and agreed to the published version of the manuscript.

**Funding:** This work was funded by the Conselho Nacional de Desenvolvimento Científico e Tecnológico (CNPq/Brazil), the Coordenação de Aperfeiçoamento de Pessoal de Nível Superior (CAPES/Brazil, Finance Code 001), by the Portuguese Science and Technology Foundation (FCT/MCT) and European Funds (PRODER/COMPETE) under the projects M-ERA-NET/0004/2015 and UIDB/04469/2020 (strategic fund), co-financed by FEDER, under the Partnership Agreement PT2020.

**Acknowledgments:** The authors wish to acknowledge the Brazilian Synchrotron Light Laboratory (LNLS) Campinas/SP for technical support in the SAXS measurements.

**Conflicts of Interest:** The authors declare no conflict of interest.

#### References

1. Santos, E.H.; Kamimura, J.A.; Hill, L.E.; Gomes, C.L. Characterization of carvacrol beta-cyclodextrin inclusion complexes as delivery systems for antibacterial and antioxidant applications. *LWT-Food Sci. Technol.* **2015**, *60*, 583–592. [[CrossRef](#)]
2. Silva, F.V.; Guimarães, A.G.; Silva, E.R.; Sousa-Neto, B.P.; Machado, F.D.; Quintans-Júnior, L.J.; Arcanjo, D.D.; Oliveira, F.A.; Oliveira, R.C. Anti-inflammatory and anti-ulcer activities of carvacrol, a monoterpene present in the essential oil of oregano. *J. Med. Food* **2012**, *15*, 984–991. [[CrossRef](#)] [[PubMed](#)]
3. Kumar, D.; Rawat, D.S. Synthesis and antioxidant activity of thymol and carvacrol based Schiff bases. *Bioorg. Med. Chem. Lett.* **2013**, *23*, 641–645.
4. Aeschbach, R.; Löliger, J.; Scott, B.; Murcia, A.; Butler, J.; Halliwell, B.; Aruoma, O. Antioxidant actions of thymol, carvacrol, 6-gingerol, zingerone and hydroxytyrosol. *Food Chem. Toxicol.* **1994**, *32*, 31–36. [[CrossRef](#)]
5. Guimarães, A.G.; Xavier, M.A.; de Santana, M.T.; Camargo, E.A.; Santos, C.A.; Brito, F.A.; Barreto, E.O.; Cavalcanti, S.C.; Antonioli, Â.R.; Oliveira, R.C. Carvacrol attenuates mechanical hypernociception and inflammatory response. *Naunyn-Schmiedeberg's Arch. Pharmacol.* **2012**, *385*, 253–263.
6. De Sousa, D.P. Analgesic-like activity of essential oils constituents. *Molecules* **2011**, *16*, 2233–2252. [[CrossRef](#)]
7. Mueller, R.H.; Maeder, K.; Gohla, S. Solid lipid nanoparticles (SLN) for controlled drug delivery—A review of the state of the art. *Eur. J. Pharm. Biopharm.* **2000**, *50*, 161–177. [[CrossRef](#)]
8. Belda-Galbis, C.M.; Leufvén, A.; Martínez, A.; Rodrigo, D. Predictive microbiology quantification of the antimicrobial effect of carvacrol. *J. Food Eng.* **2014**, *141*, 37–43. [[CrossRef](#)]
9. De Amorim Santos, I.G.; Scher, R.; Rott, M.B.; Menezes, L.R.; Costa, E.V.; de Holanda Cavalcanti, S.C.; Blank, A.F.; dos Santos Aguiar, J.; da Silva, T.G.; Dolabella, S.S. Amebicidal activity of the essential oils of *Lippia* spp. (*Verbenaceae*) against *Acanthamoeba polyphaga* trophozoites. *Parasitol. Res.* **2016**, *115*, 535–540. [[CrossRef](#)]
10. De Melo, J.O.; Bitencourt, T.A.; Fachin, A.L.; Cruz, E.M.O.; de Jesus, H.C.R.; Alves, P.B.; de Fátima Arrigoni-Blank, M.; de Castro Franca, S.; Belebony, R.O.; Fernandes, R.P.M. Antidermatophytic and antileishmanial activities of essential oils from *Lippia gracilis* Schauer genotypes. *Acta Trop.* **2013**, *128*, 110–115. [[CrossRef](#)]

11. Pastor, J.; García, M.; Steinbauer, S.; Setzer, W.N.; Scull, R.; Gille, L.; Monzote, L. Combinations of ascaridole, carvacrol, and caryophyllene oxide against *Leishmania*. *Acta Trop.* **2015**, *145*, 31–38. [[CrossRef](#)] [[PubMed](#)]
12. Bilia, A.R.; Piazzini, V.; Guccione, C.; Risaliti, L.; Asprea, M.; Capecchi, G.; Bergonzi, M.C. Improving on Nature: The Role of Nanomedicine in the Development of Clinical Natural Drugs. *Planta Med.* **2017**, *83*, 366–381. [[CrossRef](#)]
13. Amato, D.N.; Amato, D.V.; Mavrodi, O.V.; Braasch, D.A.; Walley, S.E.; Douglas, J.R.; Mavrodi, D.V.; Patton, D.L. Destruction of Opportunistic Pathogens via Polymer Nanoparticle-Mediated Release of Plant-Based Antimicrobial Payloads. *Adv. Healthc. Mater.* **2016**, *5*, 1094–1103. [[CrossRef](#)] [[PubMed](#)]
14. Keawchaon, L.; Yoksan, R. Preparation, characterization and in vitro release study of carvacrol-loaded chitosan nanoparticles. *Colloids Surf. B Biointerfaces* **2011**, *84*, 163–171. [[CrossRef](#)]
15. Zielinska, A.; Martins-Gomes, C.; Ferreira, N.R.; Silva, A.M.; Nowak, I.; Souto, E.B. Anti-inflammatory and anti-cancer activity of citral: Optimization of citral-loaded solid lipid nanoparticles (SLN) using experimental factorial design and LUMiSizer(R). *Int. J. Pharm.* **2018**, *553*, 428–440. [[CrossRef](#)]
16. Carbone, C.; Martins-Gomes, C.; Caddeo, C.; Silva, A.M.; Musumeci, T.; Pignatello, R.; Puglisi, G.; Souto, E.B. Mediterranean essential oils as precious matrix components and active ingredients of lipid nanoparticles. *Int. J. Pharm.* **2018**, *548*, 217–226. [[CrossRef](#)] [[PubMed](#)]
17. Severino, P.; Andreani, T.; Chaud, M.V.; Benites, C.I.; Pinho, S.C.; Souto, E.B. Essential oils as active ingredients of lipid nanocarriers for chemotherapeutic use. *Curr. Pharm. Biotechnol.* **2015**, *16*, 365–370. [[CrossRef](#)]
18. Zielińska, A.; Ferreira, N.R.; Feliczak-Guzik, A.; Nowak, I.; Souto, E.B. Loading, release profile and accelerated stability assessment of monoterpenes-loaded solid lipid nanoparticles (SLN). *Pharm. Dev. Technol.* **2020**, *25*, 832–844. [[CrossRef](#)]
19. Vieira, R.; Severino, P.; Nalone, L.A.; Souto, S.B.; Silva, A.M.; Lucarini, M.; Durazzo, A.; Santini, A.; Souto, E.B. Sucupira Oil-Loaded Nanostructured Lipid Carriers (NLC): Lipid Screening, Factorial Design, Release Profile, and Cytotoxicity. *Molecules* **2020**, *25*, 685. [[CrossRef](#)]
20. Souto, E.B.; Baldim, I.; Oliveira, W.P.; Rao, R.; Yadav, N.; Gama, F.M.; Mahant, S. SLN and NLC for topical, dermal and transdermal drug delivery. *Expert Opin. Drug Deliv.* **2020**, *17*, 357–377. [[CrossRef](#)]
21. Sanchez-Lopez, E.; Espina, M.; Doktorovova, S.; Souto, E.B.; Garcia, M.L. Lipid nanoparticles (SLN, NLC): Overcoming the anatomical and physiological barriers of the eye-Part I-Barriers and determining factors in ocular delivery. *Eur. J. Pharm. Biopharm.* **2017**, *110*, 70–75. [[CrossRef](#)] [[PubMed](#)]
22. Sanchez-Lopez, E.; Espina, M.; Doktorovova, S.; Souto, E.B.; Garcia, M.L. Lipid nanoparticles (SLN, NLC): Overcoming the anatomical and physiological barriers of the eye-Part II-Ocular drug-loaded lipid nanoparticles. *Eur. J. Pharm. Biopharm.* **2017**, *110*, 58–69. [[CrossRef](#)]
23. Patidar, A.; Thakur, D.S.; Kumar, P.; Verma, J. A review on novel lipid based nanocarriers. *Int. J. Pharm. Pharm. Sci.* **2010**, *2*, 30–35.
24. Doktorovova, S.; Kovacevic, A.B.; Garcia, M.L.; Souto, E.B. Preclinical safety of solid lipid nanoparticles and nanostructured lipid carriers: Current evidence from in vitro and in vivo evaluation. *Eur. J. Pharm. Biopharm.* **2016**, *108*, 235–252. [[CrossRef](#)] [[PubMed](#)]
25. Doktorovova, S.; Souto, E.B.; Silva, A.M. Nanotoxicology applied to solid lipid nanoparticles and nanostructured lipid carriers—A systematic review of in vitro data. *Eur. J. Pharm. Biopharm.* **2014**, *87*, 1–18. [[CrossRef](#)]
26. Souto, E.B.; Zielinska, A.; Souto, S.B.; Durazzo, A.; Lucarini, M.; Santini, A.; Silva, A.M.; Atanasov, A.G.; Marques, C.; Andrade, L.N.; et al. (+)-Limonene 1,2-epoxide-loaded SLN: Evaluation of drug release, antioxidant activity and cytotoxicity in HaCaT cell line. *Int. J. Mol. Sci.* **2020**, *21*, 1449. [[CrossRef](#)]
27. Souto, E.B.; Souto, S.B.; Zielinska, A.; Durazzo, A.; Lucarini, M.; Santini, A.; Horbańczuk, O.K.; Atanasov, A.G.; Marques, C.; Andrade, L.N.; et al. Perillaldehyde 1,2-epoxide loaded SLN-tailored mAb: Production, physicochemical characterization and in vitro cytotoxicity profile in MCF-7 cell lines. *Pharmaceutics* **2020**, *12*, 161. [[CrossRef](#)]
28. Souto, E.B.; da Ana, R.; Souto, S.B.; Zielińska, A.; Marques, C.; Andrade, L.N.; Horbańczuk, O.K.; Atanasov, A.G.; Lucarini, M.; Durazzo, A.; et al. In Vitro Characterization, Modelling, and Antioxidant Properties of Polyphenon-60 from Green Tea in Eudragit S100-2 Chitosan Microspheres. *Nutrients* **2020**, *12*, 976. [[CrossRef](#)]
29. Silva, A.M.; Martins-Gomes, C.; Fangueiro, J.F.; Andreani, T.; Souto, E.B. Comparison of antiproliferative effect of epigallocatechin gallate when loaded into cationic solid lipid nanoparticles against different cell lines. *Pharm. Dev. Technol.* **2019**, *24*, 1243–1249. [[CrossRef](#)]

30. Zheng, M.; Falkeborg, M.; Zheng, Y.; Yang, T.; Xu, X. Formulation and characterization of nanostructured lipid carriers containing a mixed lipids core. *Colloids Surf. A Physicochem. Eng. Asp.* **2013**, *430*, 76–84. [[CrossRef](#)]
31. Yang, Y.; Corona, A.; Schubert, B.; Reeder, R.; Henson, M.A. The effect of oil type on the aggregation stability of nanostructured lipid carriers. *J. Colloid Interface Sci.* **2014**, *418*, 261–272. [[CrossRef](#)] [[PubMed](#)]
32. Rosiaux, Y.; Jannin, V.; Hughes, S.; Marchaud, D. Solid lipid excipients—Matrix agents for sustained drug delivery. *J. Control. Release* **2014**, *188*, 18–30. [[CrossRef](#)]
33. Souto, E.B.; Almeida, A.J.; Müller, R.H. Lipid Nanoparticles (SLN<sup>®</sup>, NLC<sup>®</sup>) for Cutaneous Drug Delivery: Structure, Protection and Skin Effects. *J. Biomed. Nanotechnol.* **2007**, *3*, 317–331. [[CrossRef](#)]
34. Souto, E.B.; Doktorovova, S. Chapter 6—Solid lipid nanoparticle formulations pharmacokinetic and biopharmaceutical aspects in drug delivery. *Methods Enzymol.* **2009**, *464*, 105–129. [[CrossRef](#)]
35. Attama, A.; Schicke, B.; Müller-Goymann, C. Further characterization of theobroma oil–beeswax admixtures as lipid matrices for improved drug delivery systems. *Eur. J. Pharm. Biopharm.* **2006**, *64*, 294–306. [[CrossRef](#)]
36. Fundarò, A.; Cavalli, R.; Bargoni, A.; Vighetto, D.; Zara, G.P.; Gasco, M.R. Non-stealth and stealth solid lipid nanoparticles (SLN) carrying doxorubicin: Pharmacokinetics and tissue distribution after iv administration to rats. *Pharmacol. Res.* **2000**, *42*, 337–343. [[CrossRef](#)] [[PubMed](#)]
37. Severino, P.; Pinho, S.C.; Souto, E.B.; Santana, M.H. Polymorphism, crystallinity and hydrophilic–lipophilic balance of stearic acid and stearic acid–capric/caprylic triglyceride matrices for production of stable nanoparticles. *Colloids Surf. B Biointerfaces* **2011**, *86*, 125–130. [[CrossRef](#)]
38. Attama, A.A.; Müller-Goymann, C.C. Effect of beeswax modification on the lipid matrix and solid lipid nanoparticle crystallinity. *Colloids Surf. A Physicochem. Eng. Asp.* **2008**, *315*, 189–195. [[CrossRef](#)]
39. Gaillard, Y.; Mija, A.; Burr, A.; Darque-Ceretti, E.; Felder, E.; Sbirrazzuoli, N. Green material composites from renewable resources: Polymorphic transitions and phase diagram of beeswax/rosin resin. *Thermochim. Acta* **2011**, *521*, 90–97. [[CrossRef](#)]
40. Talens, P.; Krochta, J.M. Plasticizing effects of beeswax and carnauba wax on tensile and water vapor permeability properties of whey protein films. *J. Food Sci.* **2005**, *70*, E239–E243. [[CrossRef](#)]
41. Baek, J.-S.; So, J.-W.; Shin, S.-C.; Cho, C.-W. Solid lipid nanoparticles of paclitaxel strengthened by hydroxypropyl- $\beta$ -cyclodextrin as an oral delivery system. *Int. J. Mol. Med.* **2012**, *30*, 953–959. [[CrossRef](#)] [[PubMed](#)]
42. Kheradmandnia, S.; Vasheghani-Farahani, E.; Nosrati, M.; Atyabi, F. Preparation and characterization of ketoprofen-loaded solid lipid nanoparticles made from beeswax and carnauba wax. *Nanomed. Nanotechnol. Biol. Med.* **2010**, *6*, 753–759. [[CrossRef](#)] [[PubMed](#)]
43. Galvao, J.G.; Trindade, G.G.; Santos, A.J.; Santos, R.L.; Chaves Filho, A.B.; Lira, A.A.M.; Miyamoto, S.; Nunes, R.S. Effect of Ouratea sp. butter in the crystallinity of solid lipids used in nanostructured lipid carriers (NLCs). *J. Therm. Anal. Calorim.* **2016**, *123*, 941–948. [[CrossRef](#)]
44. Kasongo, K.W.; Pardeike, J.; Müller, R.H.; Walker, R.B. Selection and characterization of suitable lipid excipients for use in the manufacture of didanosine-loaded solid lipid nanoparticles and nanostructured lipid carriers. *J. Pharm. Sci.* **2011**, *100*, 5185–5196. [[CrossRef](#)] [[PubMed](#)]
45. Chen, Z.; Cao, L.; Shan, F.; Fang, G. Preparation and characteristics of microencapsulated stearic acid as composite thermal energy storage material in buildings. *Energy Build.* **2013**, *62*, 469–474. [[CrossRef](#)]
46. Haywood, A.; Glass, B.D. Pharmaceutical excipients—Where do we begin. *Aust. Prescr.* **2011**, *34*, 112–114. [[CrossRef](#)]
47. Higuera, L.; López-Carballo, G.; Gavara, R.; Hernández-Muñoz, P. Incorporation of hydroxypropyl- $\beta$ -cyclodextrins into chitosan films to tailor loading capacity for active aroma compound carvacrol. *Food Hydrocoll.* **2015**, *43*, 603–611. [[CrossRef](#)]
48. Chorilli, M.; Campos, G.R.; Bolfarini, P.M. Desenvolvimento e estudo da estabilidade físico-química de emulsões múltiplas A/O/AEO/A/O acrescidas de filtros químicos e manteiga de karité. *Lat. Am. J. Pharm.* **2009**, *28*, 936–940.
49. Martins, A.J.; Cerqueira, M.A.; Fasolin, L.H.; Cunha, R.L.; Vicente, A.A. Beeswax organogels: Influence of gelator concentration and oil type in the gelation process. *Food Res. Int.* **2016**, *84*, 170–179. [[CrossRef](#)]
50. Alexandridis, P.; Olsson, U.; Lindman, B. A record nine different phases (four cubic, two hexagonal, and one lamellar lyotropic liquid crystalline and two micellar solutions) in a ternary isothermal system of an amphiphilic block copolymer and selective solvents (water and oil). *Langmuir* **1998**, *14*, 2627–2638. [[CrossRef](#)]

51. Shah, R.M.; Bryant, G.; Taylor, M.; Eldridge, D.S.; Palombo, E.A.; Harding, I.H. Structure of solid lipid nanoparticles produced by a microwave-assisted microemulsion technique. *RSC Adv.* **2016**, *6*, 36803–36810. [[CrossRef](#)]
52. DeSouza, A.L.R.; Andreani, T.; Nunes, F.M.; Cassimiro, D.L.; de Almeida, A.E.; Ribeiro, C.A.; Sarmiento, V.H.V.; Gremião, M.P.D.; Silva, A.M.; Souto, E.B. Loading of praziquantel in the crystal lattice of solid lipid nanoparticles. *J. Therm. Anal. Calorim.* **2012**, *108*, 353–360. [[CrossRef](#)]



© 2020 by the authors. Licensee MDPI, Basel, Switzerland. This article is an open access article distributed under the terms and conditions of the Creative Commons Attribution (CC BY) license (<http://creativecommons.org/licenses/by/4.0/>).